International Conference
1ST International Conference on Innovations, Recent Trends and Challenges in Mechatronics, Mechanical Engineering and New High-Tech Products Development
MECAHITECH'09

Bucharest, 8-9 October 2009

Tribological Characteristics Improvements of Hip Prostheses Using Nanostructured Coatings

L. L. Badita[1, 2], L. Capitanu[2]
1. Micro and Nanomechatronic Technolologies Laboratory, National Institute for Research and Development in Precision Mechanics Bucharest, Romania
2. Romanian Academy – Institute of Solid Mechanics, Bucharest, Romania

ABSTRACT

The aim of this project is to improve tribological properties of hip prostheses that deteriorate due to the high superficial pressures produced by mechanical movements of the body. They may be used for different periods of time, depending on its composition and properties.

This project began with theoretical studies on sphere/plane thimbles, which simulated the femural head and acetabular cup. Using these devices we study the tribological properties of hip prostheses; determine the wear factor, the volume of material and the medium depth of the layer removed by wear process. In order to obtain a resistant Ti-6Al-4V hip prosthesis, with high mechanical properties, the used heads will be coated with nanostructured coatings. Surface's topography of the femoral head covered with nanostructures, after movements in the acetabular cup is important due to qualitative and quantitative information. Structural investigations are carried out by atomic force microscopy (AFM). This study may be useful for the identification of scratching and wear mechanisms generation.

KEYWORDS: Hip prosthesis, Nanocoatings, Tribological properties, Wear factor, Atomic Force Microscopy

1. INTRODUCTION

The hip is essentially a ball and socket joint, formed by the articulation of the rounded head of the femur and the cup-like acetabulum of the pelvis. It forms the primary connection between the bones of the lower limb and the axial skeleton of the trunk and pelvis. The cup-like acetabulum forms at union of three pelvic bones and the joint may not be fully ossified under the age of 25 years. The large head of the femur attaches directly to the acetabulum. The head of the femur is attached to the shaft by a thin neck region that is often prone to fracture in the elderly, mainly due to the degenerative effects of osteoporosis.

Six different kinds of movements are possible in the hip joint: flexion and extension (on or from the spine and on or from the thigh), abduction and adduction of the femur, internal (medial) and external (lateral) rotation of the pelvis, thigh or spine (see figure 1).

Accidents produced by the simplest ways can have blasting results. For this reason people replace the damaged bones by different prostheses, in this case a total hip endoprostheses. The total hip prosthesis consists of three parts (see figure 2):

- a cup that replaces the hip socket;
- metallic encasing;
- a ball that will replace the fractured head of the femur;

- a stem that is attached to the shaft of the bone to add stability to the prostheses.

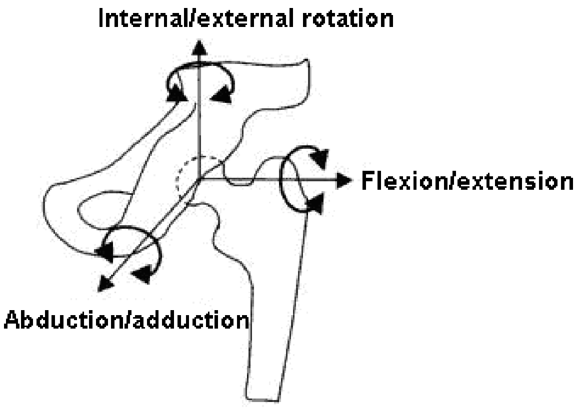

Figure 1: Movements in the hip joint.

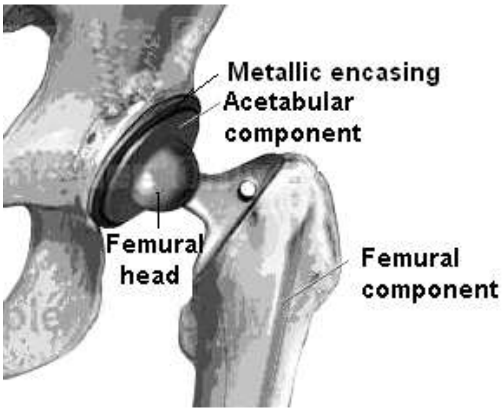

Figure 2: Components of a total hip prosthesis

These systems deteriorate due to the high superficial pressures produced by mechanical movements of the body. Taking into account the hip prostheses components, there can be wear acetabulat cup – ball wear and acetabular cup – encasing wear.

Beside this, the entire system may be used for different periods of time, depending on its composition (ceramic, metals) and properties. After exclusion of hip prostheses from the human body, it was observed numerous scratches. Such scratching may be attributed to wear resulting in loss of material or plastic deformation of the surface without loss of material.

2. WEAR MECHANISMS

The deterioration process has a complex mechanism, combining abrasive wear, adhesive wear, third body wear and fatigue wear (see figure 3).

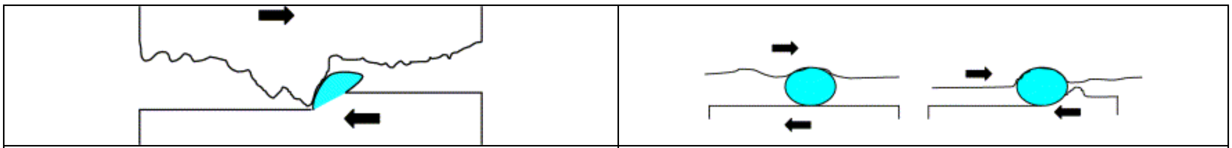

(a) Abrasive wear mechanism

(c) Third body wear mechanism

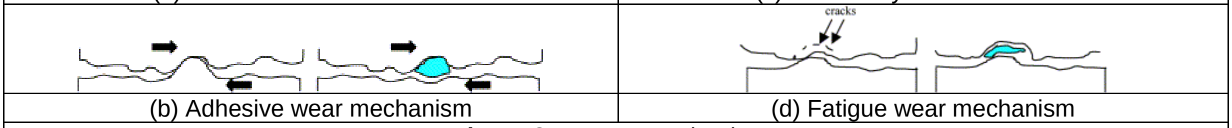

(b) Adhesive wear mechanism

(d) Fatigue wear mechanism

Figure 3: Wear mechanisms

Abrasive wear is removal of material from one surface by the other. Local high points or “asperities” on the surface of the harder material will gouge into the softer material and produce wear particles.

Adhesive wear is where localized bonding of the two surfaces occurs such that the attachment force is stronger than the yield strength of the material and a small piece of material is removed from one surface and is attached to the other. This process leaves small pits in the surface and can lead to “transfer films” of polymer on the metal surfaces which are occasionally observed.

In the third body wear the damage is caused by a particle caught between the two surfaces. These third bodies can become embedded in the UHMWPE and lead to scratching of the metal counter face which, in turn, leads to accelerated abrasive wear.

Fatigue wear can lead to subsurface cracks propagating and flaking off of particles from the surface. High subsurface stresses can also be caused by third bodies between the two articulating surfaces leading to accelerated fatigue wear.

3. MATERIALS USED FOR HIP PROSTHESES

In these conditions, it is necessary to have a resistant prosthesis, with anticorrosive composition and high mechanical properties. In order to improve mechanical properties of prosthesis, these have been coated, during the years, with different materials, which have superior properties. There are experiments made with amorphous carbon coatings (diamond like carbon, hydrogenated amorphous carbon).

Materials engineers must consider the physiologic loads placed on the implants. Material choices also must take into account immune system biocompatability, the environment, corrosion issues, friction and wear of the articulating surfaces, implant fixation either through osseointegration (the degree to which bone will grow next to or integrate into the implant) or bone cement.

One of the major problems for these devices is materials-related: wear of the polymer cup in total joint replacements. Stainless steel, titanium alloy, polymers and ceramic composites undergo degradation after 10–15 years of use. The body’s immune system attempts, unsuccessfully, to digest the wear particles. Enzymes are released that eventually result in the death of adjacent bone cells, or osteolysis. This represents an important problem in total hip arthroplasty generated through different materials, often leading to component loosening, bone loss, pathologic fractures, and complex revision surgery. Femoral bone weakened by osteolysis can fracture under high loading conditions and require replacement. Examples of osteolysis presumed to be caused by wear debris of devices include bone resorbtion around failed elastomeric finger, tow, and wrist prostheses and around failed poly(tetrafluoroethylene)-carbon fiber temporomandibular joint (jaw) prostheses. Over time, sufficient bone is resorbed around the implant to cause mechanical loosening which necessitates an implant replacement or revision. When present in sufficient amounts, particulates generated by wear, fretting, or fragmentation induce formation of an inflammatory, foreign-body granulation tissue that has the ability to invade the bone–implant interface. This may result in progressive loss of bone, that threatens the fixation of prostheses inserted with or without cement. The corrosive attack results in metal release and mechanical failure of the joint component.

Zirconium alloy substrate is relatively soft when compared with cobalt-chrome alloy femoral heads and may deform in contact with acetabular shell materials in the case of dislocation. Cobalt-chrome alloy femoral heads articulating with ultra-high molecular weight polyethylene acetabular liners have been the main stay of hip arthroplasty for more than 30 years. Ceramics, with extremely low wear rates, remain a risk of catastrophic failure because of the inherently low fracture toughness of the materials. Metal-on-metal bearings, metal allergy and bioactive wear debris are still considered clinical issues. Oxinium components have a unique ceramic layer (4 µm thick) to mitigate against wear, akin to a zirconia ceramic material, and have an integral metal substrate that provides toughness and high fatigue strength.

Many conventional wear-resistant or corrosion-resistant materials are difficult to apply in those environments, which are subjected to the combined effects of mechanical wear and chemical attack. Metal–matrix composite (MMC) coatings reinforced with hard ceramic particles are promising materials for improvement in various mechanical properties over conventional monolithic alloys.

Metallic implants are generally used for load bearing applications. A thin hydroxyapatite (HA) coating, having the composition $Ca_{10}(PO_4)_6(OH)_2$ similar to bone apatite, can prevent the release of metal ions from the substrate into the biological environment. HA coatings on metallic substrates suffer from many problems like cracking and peeling off, which results in the release of harmful metal ions to the body environment. The adherence of the HA coating to the substrate is very poor. In order to overcome inferior adhesion an interlayer coating can be provided in between the metal substrate and the HA outer layer.

In a physiological environment, metallic, ceramic, or polymeric wear particles may be trapped between two moving surfaces, causing three-body wear, which generally causes a significantly higher wear rate than two-body wear. This wear may cause loosening of the prostheses by the resulting poor mechanical fit between the ball and socket of the hip. Generation of wear debris is an important factor both because of the potential for wear debris to migrate to distant organs, and because of local physiological responses such as inflammatory, cytotoxic, and osteolytic reactions.

Taking into account all these studies realized in the last years, the most common failures of hip prostheses are:

- Surgical problems (e.g., problematic orientation or problems in wound healing)
- Host abnormalities or diseases (e.g., osteopenia)
- Infection
- Material fracture, wear, and corrosion.

For these reasons we are trying to improve tribological properties of hip prosthesis using nanostructured coatings and to characterize its surface by a microscopic technique.

4. TECHNIQUES FOR THIN FILMS DEPOSITION

The most common methods for deposition of a coating layer are: physical vapour deposition, chemical vapour deposition, thermal spraying. Plasma electrolytic oxidation can also be used to create hard coatings on metal substrates.

Physical vapour deposition (PVD) involves the generation of positively charged ions of various metals, which are evaporated from a solid target. These metal ions react with gas ions that are introduced into the chamber in order to create various compositions. The parts to be coated are given a negative bias in order to attract the positively charged ions. The result is a strong mechanical bond between the coating and the substrate. The coatings produced have typically 1–5 µm thickness.

Chemical vapors deposition (CVD) involves transforming gaseous precursors into a solid material which is deposited as a solid surface layer. Precursor gases diluted in carrier gases are delivered into the reaction chamber at approximately ambient temperatures. As they come into contact with a heated substrate, they react forming a solid phase, which is deposited onto the substrate. This process allows coating of all surfaces of a component and can produce coatings typically with 3–12 μm thickness. The primary difference between CVD and PVD is that in a CVD process the reaction takes place at the surface and in PVD the reaction takes place in the atmosphere and the bulk compound is then deposited on the surface.

Thermal spraying involves introduction of small particles of the coating material into a flame such that they are propelled against the target surface with sufficient kinetic energy to form a strong bond with the substrate.

Plasma electrolytic oxidation (PEO) transforms the metal surface using plasma discharge in a liquid electrolyte, to form a layer of hard and dense ceramic material on the surface. This process is mainly used on the light alloys (e.g. magnesium, titanium, aluminium and zirconium) and can form layers from a few micrometers to over 100 μm thickness.

5. STUDY AND CHARACTERIZATION TECHNIQUES

Wear processes occurring inside different prostheses are an important source of debris, but these changes are often impossible to see with the naked eye. A methodology of ascending degrees of resolution was established using macroscopic (resolution millimeters), microscopic (resolution microns) and nanoscale (resolution nanometers) measurements. During the years different methods of investigation were used to establish the surface topography and any evidence of changes to the topography of these.

For example, stems were assessed by plain visual examination and light microscopy.

In some studies have been performed microscopic investigations of the articulating surfaces of the early explants of highly cross-linked polyethylene liners using optical microscopy. The articulating surfaces of all acetabular liners were analyzed and documented by optical microscopy using an Olympus SZX12 optical microscope with a coaxial illuminator. The main result was the observation of small scratching, heavy scratching, polishing, and presence of machining marks. Machining marks are some regular circular or radial lines generated on machined surfaces during the fabrication of the implant. Another optical microscope (Olympus SZ 61) was also used for evaluation of re-growth morphology and of the surface morphology of the coatings.

For simple cobalt-chrome heads a stereo microscope revealed predominantly roughening, scratching, metallic transfer and micro-ploughing. Depths of scratches on the cobalt-chrome heads were measured using microscopy techniques. Deformed material raised above the bearing surface of cobalt-chrome heads or oxinium was only discernible using such a technique.

Measurement systems for 3-D surface topography may be characterized by the physical principle used in the surface-sensor interaction. Profilometric 3-D instruments may be either contacting or noncontacting. The former, use a stylus to trace the contours of a surface and are limited by the geometry of the stylus. It may be unable to register narrow or deep grooves within surface topography. The WYKO NT 2000 (WYKO NT 2000 Veeco, Tucson, AZ) interferometer is a noncontacting optical instrument that uses the interference patterns of light reflected by a surface to measure surface topography. The accuracy of this method is limited only by the wavelength of the light used for assessment.

3-D Interference Microscopy, another important technique for the measurement of surface topography, provides quantitative information at a nanometer scale, surface mapping and parametric analysis.

X-ray photoelectronspectroscopy analysis is another method used for topographic characterization of coated surfaces. It was used to evaluate the valence state of Ti atoms and the O/Ti ratio; employed to analyze the chemical composition and structure of electrochemically passive film formed by a composite.

X-ray diffraction (XRD) is used to investigate structural properties, performed with a DRON-2 powder diffractometer with Fe-filtered CoKa radiation. The average size of crystallites can be calculated based on XRD spectra in a conventional way according to the Scherrer formula. The composition of ZnP and ZnP/HA coatings were characterized based on XRD analysis Shibli et. All

The composition and microstructure of the nano-SiO_2 particles reinforced Ni-based composite alloying layer were analyzed by using XRD, TEM (Transmission Electron Microscopy) and SEM (Scanning Electron Microscopy). Using TEM, nanoparticles can be observed with difficulty because of insufficient contrast for their size, which has to be smaller than the thickness of the thin section investigated (typically about 60 nm).

UHMWPE wear nanoparticles were revealed by scanning electronic microscopy with field emission gun (FEGSEM) in periprosthetic tissues of two different patients.

UHMWPE wear particles are a major cause of long-term failure of total hip replacements. UHMWPE particles size varies from less than 1 μm to several millimeters, but particles with less than 10 μm have the highest biological activity. Some wear particles in vitro produced in hip simulators have been shown to be less than 0.2 μm. Recently, it was observed in vitro more particles tending to nanometric sizes. In vivo wear occurring nanoscale particles with sizes below 0.05 μm.

UHMWPE wear particles were detected in vivo tissues obtained during periprosthetic revisions of hip prosthesis. Were cut two small amounts of tissue, dry, frozen and soaked in a mixture of chloroform and methanol for 12 h. The solvent was decanted. After the second decantation, the tissue samples were dried in a stream of dry air and heated for 2h at 60°C. Were processed more periprosthetic tissue samples, determining the total amount and morphology of wear particles. It was found that the periprosthetic tissue contains more wear particles of nanometric size. In order to study these particles, membranes of polycarbonate (PC) with polyethylene wear particles isolated were fixed in a metal sheet with a conductive paste of Ag, and the samples were covered by sputtering with a platinum layer of 10 mm thick. This restraint is necessary to remove the damage of the sample and taken of particles by the current at very high E field produced by cannon needed to detect nanoparticles.

Observed nanoparticles are pure UHMWPE. In all cases were found peaks only for C (possible from PC membrane and partly from PE particles), O (PC membrane), Pt (10 nm thickness of the platinum layer deposited by vacuum sputtering), Ag and Cl (from the conductive paste of Ag which has set menbrana on hard). There was no-one from the other elements that may indicate fragments of bone (Ca, P), powder (Si), organic impurities (N), metallic wear particles (Cr, Mo, Ti), ceramic wear (Al, Zr).

Fig. 4 presents the PC membrane with PE particles isolated from periprosthetic tissue of a patient with an implant of 8.5 years. On the membrane, nanometric wear particles tend to form aggregates (Fig. 4a, 4c and 4e), which can be distinguished by sonic separation of the filtered suspension (Fig. 4b, 4d and 4f).

Aggregates of nanoparticles with average size, not sonically separated (Fig. 4a; enlarge x 7500) and large size (Fig. 4c; enlarge x 12,000), shows that like themselves are microparticles. Single nanoparticles of the aggregate could be observed only at medium zoom. The magnified (Fig. 4d), single nanoparticles can be clearly observed. Micrographs of nanoparticles sonically separated, at high zoom (Fig. 4f) are appropriate for image analysis.

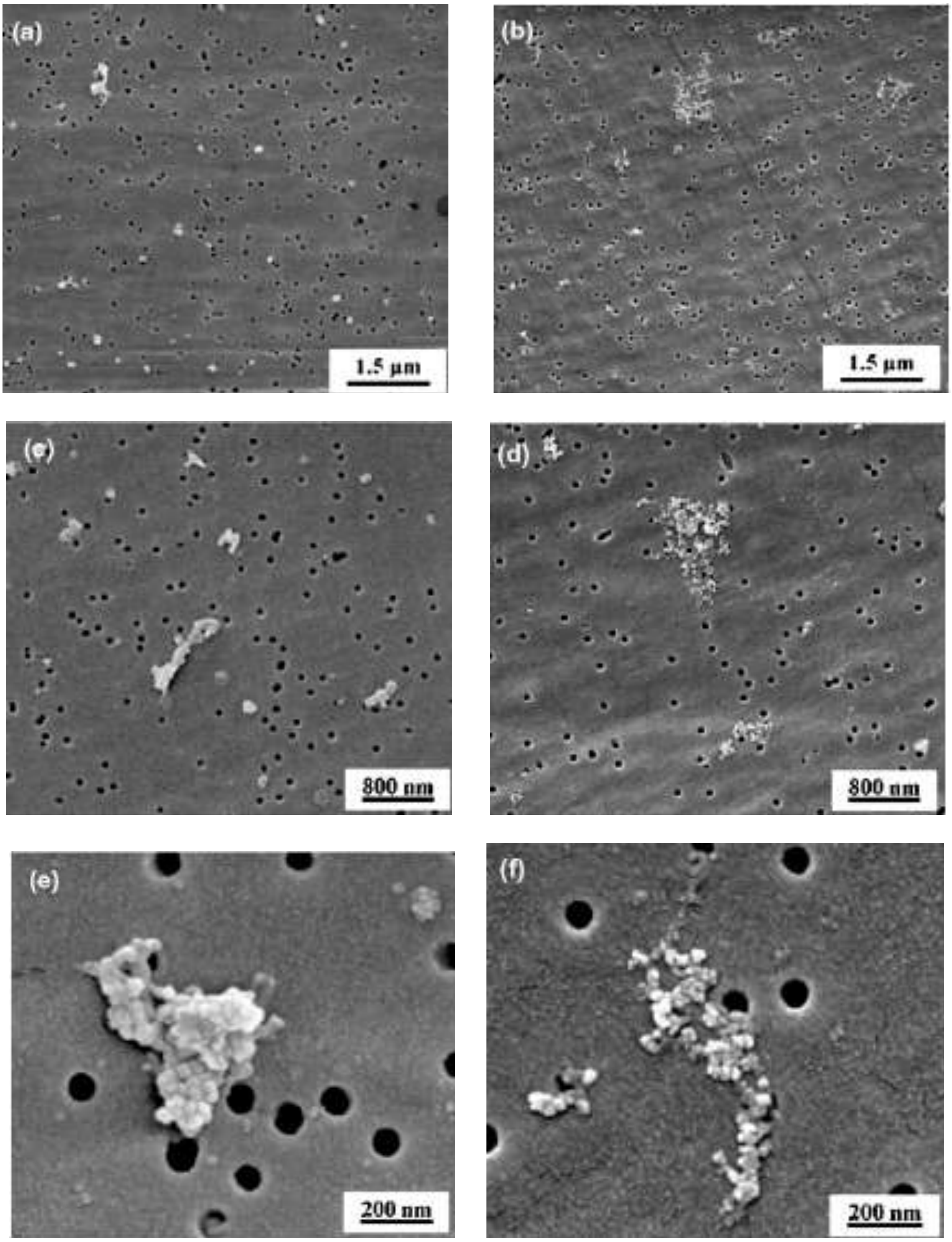

Figure 4. Microfotografii FEGSEM micrographs of UHMWPE particles by a 0.1 µm PC membrane. Left column (a, c and e): particles without sonic washing before filtering; the right column (b, d and f): particles sonic washed before filtration. Selected micrographs were made with medium zoom (a and b), large (c and d) and high (e and f).

A SEM HITACHI S-2400 was used to analyze the surface morphology of some other coatings, like HA coating developed on the ZnP coated substrate. The HA coated coupons were rinsed with acetone, dried in air and its surface was gold coated in order to make it conductive during the SEM analysis.

Besides all these techniques, atomic force microscopy is a popular method for these types of studies. AFM was used, for example, to characterize the uniformity and grain size of TiO_2 or nanostructured films deposited on femoral head's substrates.

6. EXPERIMENTAL AND THEORETICAL STUDIES

This project began with some theoretical and experimental studies on sphere/plane samples, which simulated the femural head and acetabular cup. In the present case, the plane is the acetabular cup pressed by the spherical head, which destroys, in time, the prostheses.

Using such a device and considering a vertical and static charge, there is possible to study the tribological properties of hip prostheses.

Taking into account technical constraints, applications for these studies were considered practically constant. After these studies, the used disks will be coated using vapor deposition (chemical or physical) with standard and nanostructured coatings (titanium nitride TiN, chromium nitride CrN, chromium oxide Cr_2O_3), because these materials offer the opportunity to improve mechanical properties of prosthesis. The hip prosthesis was made up of Ti-6Al-4V, the stiffness of titanium being close to that of bone. Two bodies with a contact point strain when one of these is pressed on the other, resulting a small contact surface. The settled formulas show that on this contact surface only the normal tensions action.

Defining equivalent elasticity module:

$$E = \frac{2E_1E_2}{\left(1-\nu_1^2\right)E_2 + \left(1-\nu_2^2\right)E_1} \qquad (1)$$

and equivalent contact radius:

$$r = \frac{r_1 r_2}{r_2 - r_1} \qquad (2)$$

for two bodies in contact and folowing the demonstration presented in a previous authors article few characterization parameters are obtained.

The sphere penetrating the plane surface under the influence of the vertical charge will produce a wear trace in this material (see figure 5). External dimensions of obtained imprint (length *L* and width *l*) are measured using an optical microscope.

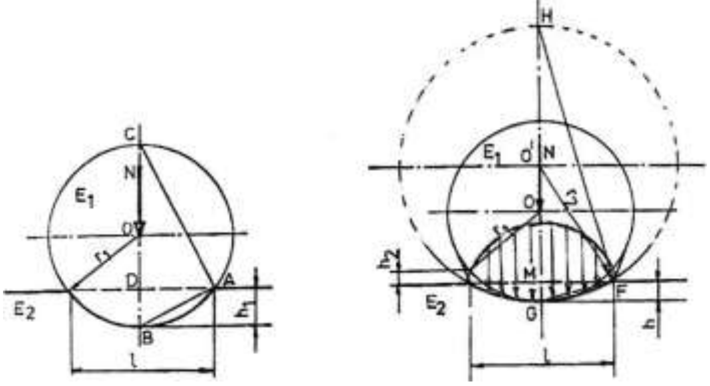

Figure 5: Radius of deformed area.

The volume of material removed by wear will be:

$$V_u = \sum_{i=1}^{n} S_i p_i = 2\, l_m\, h_m\, \mathbf{L}/3 \qquad (3)$$

where S_i – lateral surface of a cylindrical sector, l_m is the medium width of the wear imprint; h_m is the medium depth, and L is the length of the wear imprint.

It is necessary to measure the width of the imprints in 5 points established before using a microscope and to calculate the medium width of the wear imprint. Using this value it is possible to calculate the volume of material removed by wear process and the medium depth of the layer removed by wear.

Wear factor was determined using the Archard relation:

$$V_u = kFvt \qquad (4)$$

where V_u is volume of material removed by wear (cm^3); F is the load (daN); v is the relative sliding speed (cm/s); t is time of the experiment (h) , and k is the wear factor ($cm^3 s/daNmh$). By dividing both terms of the previous relation with the contact area A, it will give the relation:

$$V_u/A = kvtF/A \qquad (5)$$

$$h_u = kpvt \qquad (6)$$

where h_u is the depth of the worn material layer (cm) and p is the pressure on the contact surface (daN/cm^2). This relation (6) states a general law of the wear dependence, varying with the pressure between the bodies in contact (p) and the space covered by abrasion, namely $L_f = vt$. It will result:

$$k = h_u / pvt = h_u / pL_f \qquad (7)$$

$$k = V_u / Fvt = V_u / FL_f \qquad (8)$$

Generally, it is difficult to calculate the wear factor due to difficulties to measure the volume of material removed by wear.

Before realizing the coatings and analyzing the properties of these materials, we are analyzing the hip prosthesis without any coating.

Following visual inspections, some local rubbing and a severe scratch could be located on femoral head, caused probably by a hard particle embedded in the cup. For a more accurate picture of the femoral head surface deteriorations the procedure described by Najjar et al was adopted. By intermediate of 5 parallels (from A to E) and 6 meridians (from 1 to 6) the femoral head was divided in 36 regions.

We realize hip prosthesis topography of these parts by using an atomic force microscope (NTEGRA Probe Microscope - figure 6) working in the contact mode. AFM images are processed using Nova SPM software.

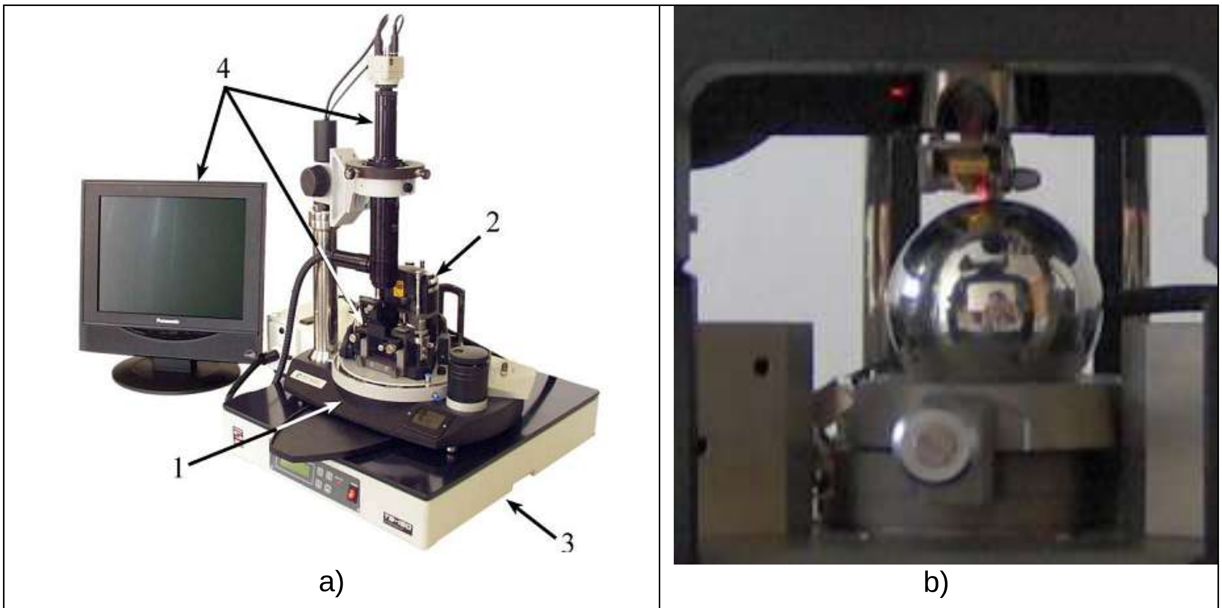

a) b)

Figure 6: NTEGRA Probe NanoLaboratory: a)1 – base unit; 2 – measuring head; 3 – vibration isolation system; 4 – optical viewing system; b) detail of the AFM probe

7. RESULTS

The results of some experimental tests of wear of the acetabular cups, based on gravimetric measurements are listed in table 1 or 2 and plotted in figure 8 or 9. In table 1 are listed the values of wear rate resulted from experiments as gravimetric wear rate (10^{-11} *g/mm* of the length of entire travel) and volumetric wear rate also (10^{-7} *mm*^{3}*/mm* of the length of entire travel). One could notices that in the dry friction case the wear rate is significantly increased as for lubricated friction (with physiological serum), both for small and doubled relative sliding speed. When the sliding speed used in the experiment has a doubled value, it can be observed that the wear rate values are smaller than before, both for dry friction and physiological serum friction.

The diagrams in figure 7 show that the dependence between the wear rate and the contact pressure is exponential, this rate being doubled by the absence of lubrication.

p *MPa*	v *cm/min*	L_f 10^6 *mm*	Dry friction			In physiological serum		
			Wear	Wear rate		Wear	Wear rate	
			10^{-5} g	10^{-11} *g/mm*	10^{-7} *mm*^{3}*/mm*	10^{-5} g	10^{-11} *g/mm*	10^{-7} *mm*^{3}*/mm*
0.7	527	22.02	27.90	176.277	18.955	14.10	89.086	9.579
1.4	527	22.02	79.10	445.602	47.914	38.40	242.618	26.088
2.1	527	22.02	188.90	1193.505	128.334	80.20	447.572	48.126
0.7	1055	44.04	32.30	102.038	10.972	6.90	21.798	2.344
1.4	1055	44.04	109.70	346.552	37.264	11.30	59.372	6.384
2.1	1055	44.04	348.30	837.279	90.030	14.10	89.086	9.579

Table 1: Wear rate for frictional couple Ti6Al4V + TiN / UHMWPE

p (*MPa*)	v (*cm/min*)	F_N (*N*)	Dry friction		Physiological serum	
			F_f (*N*)	μ	F_f (*N*)	μ
0.7	527	500	14.25	0.285	1.75	0.035
1.4	527	1000	32.00	0.320	4.90	0.073
2.1	527	1500	51.30	0.342	9.75	0.090
0.7	1055	500	14.00	0.280	1.60	0.085
1.4	1055	1000	29.50	0.295	4.10	0.125
2.1	1055	1500	45.00	0.300	6.75	0.141

Table 2: Frictional coefficients for frictional couple Ti6Al4V +TiN /UHMWPE

Table 2 lists the values of frictional coefficient measured for frictional couple Ti6Al4V + TiN / UHMWPE and their dependence on pressure are plotted in figure 8.

The frictional coefficient linearly increases with the load for both friction cases presented and the values in the case of dry friction are bigger. The frictional coefficient decreases when the relative speed increases. When the speed value is doubled, the coefficient has smaller values for dry friction and bigger for lubricated one. In all cases there are exponential dependences.

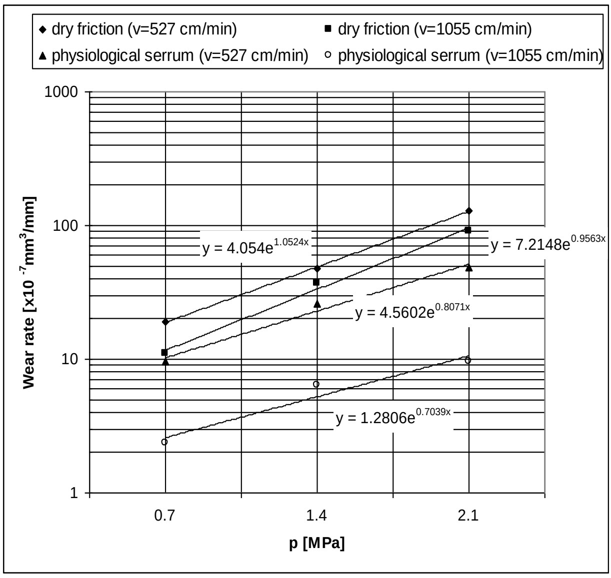

Figure 7: Wear rate vs. contact pressure in dry friction and physiological serum lubrication

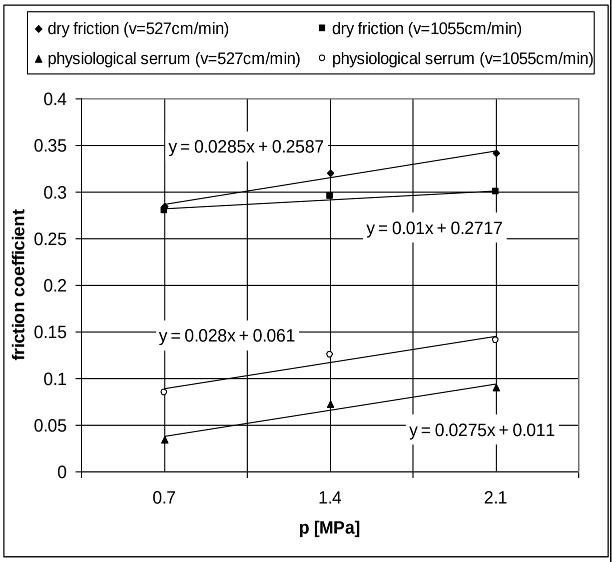

Figure 8: Friction coefficient vs Contact pressure.

Visual analysis of all the implants is not able to show delaminations or cracks on any of the surfaces. The most common surface features of both conventional and cross-linked groups of explants were fine or heavy scratching of the articulating surfaces.

Using Light Microscopy Study, three principal changes were seen on the surfaces of explanted stems: polishing, pitting, and debris. These are considered to be indicators of different wear mechanisms and in some cases could be useful to determine it.

In our case, the optical microscopy study of the 36 regions delimited on the femoral head, revealed that 25% of the entire surface has isolated micro-scratches despite of polished macroscopic aspect. In the area of intersections between 5 and 2 meridians with E, D and C parallels, some seriously damaged regions are identified covering 15-20% of the femoral head surface. A closer look to the region 6B identified an embedded wear particle which scratched the femoral head surface (figure 9a, 9b). The large scratch could be related to the abrasion due to third body, namely the wear particles. Signs of severe micro cutting were detected also in region 6B (see figure 9c). In Figure 9d one could observe small scratches and pits produced by biotribological corrosion. The corrosion pits occurred due to strong mechanical loading combined with the local temperature increase, at the contact interface.

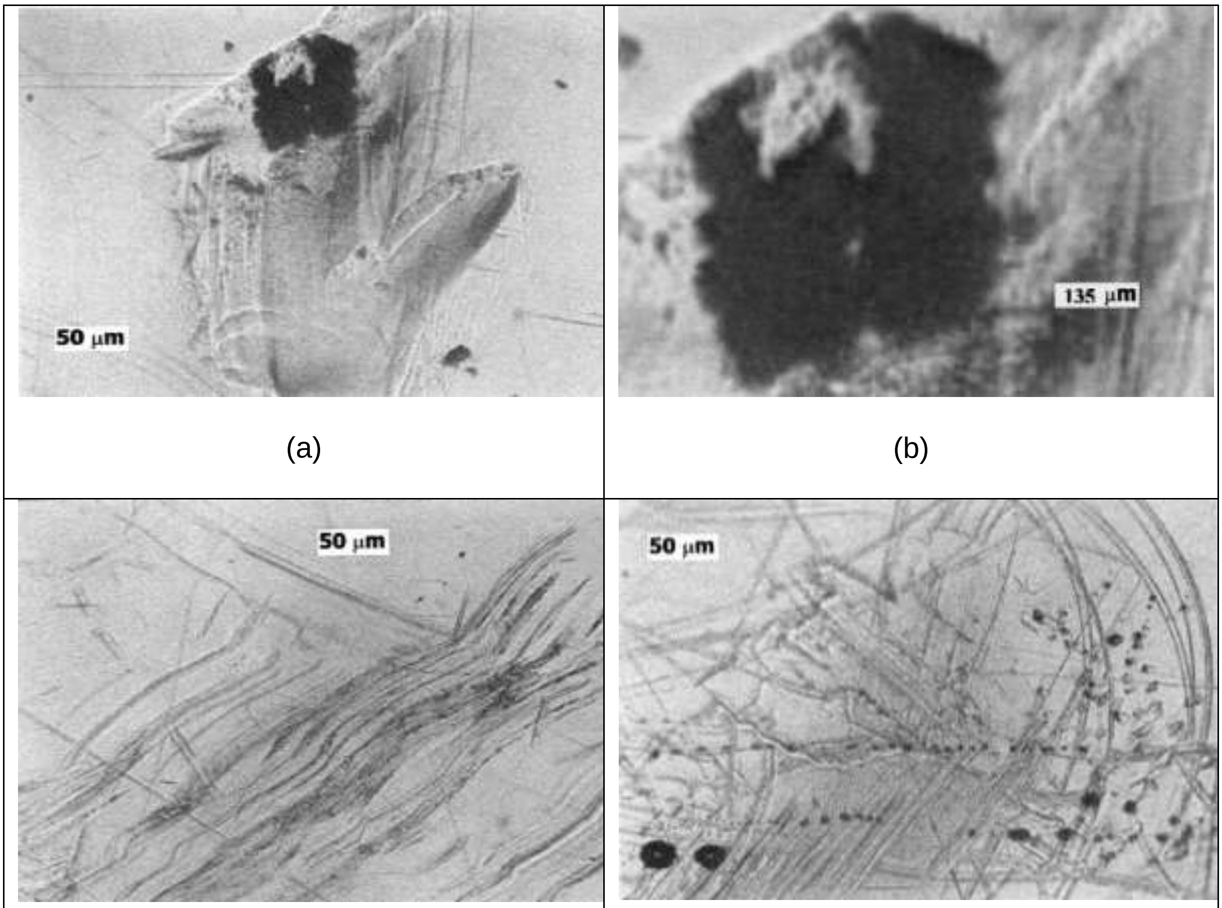

(a) (b) (c) d)

Figure 9. Scratching (a), embedded wear particle (b) and magnified image in (c) and corrosion fretting (d) of femoral head in 6B zone

Similar results were obtained also for the others parts of the prosthesis. Taking into account all these studies we shall continue the researchers and AFM microscopy studies. These could improve topographic characterization of nanostructured coatings surface.

It were observed tree special areas on the femoral head made from Ti. There are regions with a polished visual aspect, and areas with a small level of luminosity. In the second part appears a high deterioration degree, with a lot of scratches. The third category of regions covers more than 50% of the femoral head and has an intermediate level of luminosity. Here, the deterioration level is not so high.

All these topographies may be observed on an isometric diagram, registered with a 3D contact profilometer. In figure 10 are represented few examples for different zones that rise from regions having a high level, an intermediate level and a small luminosity level.

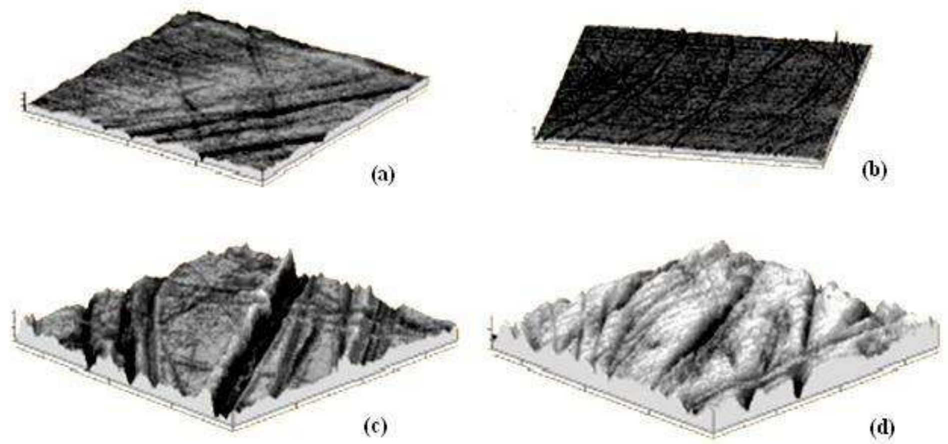

Figure 10. Isometric representations of typical zones, having (a) a high luminosity level (a), an intermmediate luminosity level (b), a small luminosity level and small scratches and material on the borders (c) and with a small luminosity level and big scratches without any kind of material on the borders (d)

Using roughness analysis it is possible to determine some parameters in order to characterize our surface (figure 11, figure 12). Besides minimal, maximal and average height of the, is possible to find out the entropy and redundance. Some important parameters are:

- Ten point height (Sz) that expresses surface roughness by the selected five maximal heights and hollows, nm
- Surface skewness (Ssk) characterizes the non-symmetry of distribution. If the asymmetry is different from zero. The distribution is non-symmetrical. The asymmetry equals to zero for the symmetrical distribution. The asymmetry is positive, if the distribution is excessive on the right and negative if the distribution is excessive on the left
- Coefficient of kurtosis (Ska) characterizes the distribution spread.

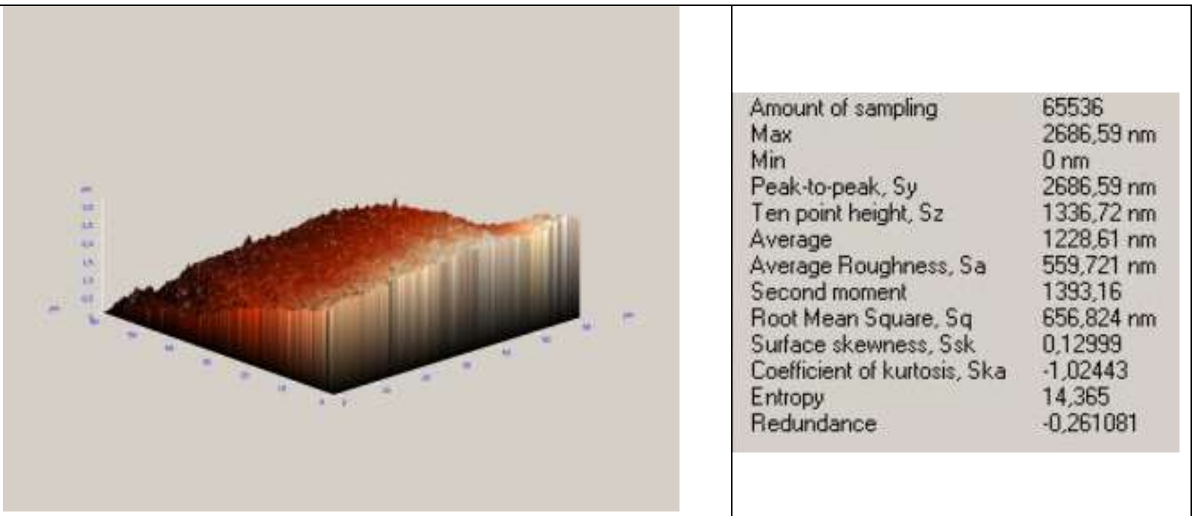

Amount of sampling	65536
Max	2686,59 nm
Min	0 nm
Peak-to-peak, Sy	2686,59 nm
Ten point height, Sz	1336,72 nm
Average	1228,61 nm
Average Roughness, Sa	559,721 nm
Second moment	1393,16
Root Mean Square, Sq	656,824 nm
Surface skewness, Ssk	0,12999
Coefficient of kurtosis, Ska	-1,02443
Entropy	14,365
Redundance	-0,261081

(a) (b)

Figure 11. 3D AFM image obtained on a femoral head in the reagion 5E (a), parameters characterizing our surface (b)

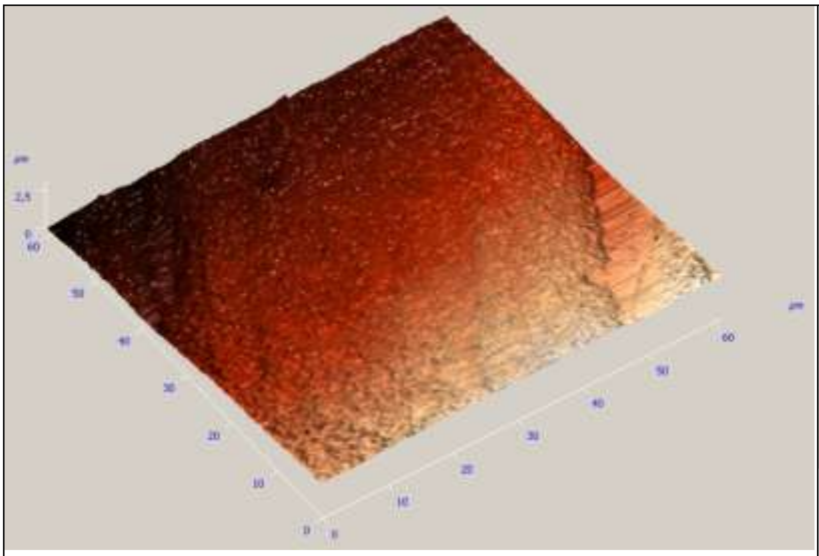

(a)

Amount of sampling	65536
Max	3091,88 nm
Min	0 nm
Peak-to-peak, Sy	3091,88 nm
Ten point height, Sz	1514,5 nm
Average	1500,9 nm
Average Roughness, Sa	534,005 nm
Second moment	1630,27
Root Mean Square, Sq	636,469 nm
Surface skewness, Ssk	0,0579796
Coefficient of kurtosis, Ska	-0,876364
Entropy	14,4027
Redundance	-0,242279

(b)

Figure 12. 3D AFM image obtained on a femoral head in the reagion 5E (a), parameters characterizing our surface (b)

8. CONCLUSIONS

As it was demonstrated in the last years, femoral head damage may occur during hip joint movements and may lead to accelerated materials wear. This is an important reason for femoral head covering, which offer the opportunity to improve system's properties. From the tribological point of view, a favorable coating material needs to exhibit an elastic modulus which is similar to that of the substrate material; and to have a good adherence to the substrate. In order to obtain a clear characterization of the coatings the study of its topography is useful. Such a study can be made by different techniques, but we decided on AFM because its images display high quality and dense nanocrystalline structure of prepared thin films.

During the years, all investigations carried out by AFM have shown a strong influence of both the substrate type, and its placement in the deposition chamber, on the structural properties of the films.

An important result is that the wear rate and friction coefficient decrease in physiological serum (natural medium) for a Ti6Al4V + TiN/UHMWPE hip prosthesis. This could help to an increase of its life period. Taking into account this observation, the main conclusion is that nanostructured coatings offer the opportunity to improve system's properties. The next steps will be based on these experiments and some other materials will be used and characterized to protect against hip prosthesis breakdown.

9. REFERENCES

[1] J. Nevelos, Surface engineering of prosthetic knee components, The Knee, 11 (2004) 163-167.

[2] W. Österle, D. Klaffke, M. Griepentrog, U. Gross, I. Kranz and Ch. Knabe, Potential of wear resistant coatings on Ti–6Al–4V for artificial hip joint bearing surfaces, Wear 264 (2008) 505-517.

[3] L. Capitanu, A. Iarovici, J. Onisoru, Tribological behaviour of a total hip prostheses during normal walking active cycle, Proceedings of Balkantrib '05, Kragujevac, Serbia, 2005, pp. 317 -323.

[4] Prem V. Pavoor, Brian P. Gearing, Orhun Muratoglu, Robert E. Cohen and Anuj Bellareb, Wear reduction of orthopaedic bearing surfaces using polyelectrolyte multilayer nanocoatings, Biomaterials, 27 (2006) 1527-1533.

[5] Howell JR Jr, Blunt LA, Doyle C, Hooper RM, Lee AJ, Ling RS, In vivo surface wear mechanisms of femoral components of cemented total hip arthroplasties: the influence of wear mechanism on clinical outcome, J Arthroplasty. 19 (2004) 88-101.

[6] Jing wen, Yang leng, Jiyong chen, Chenge zhang, Chemical gradient in plasma-sprayed HA coatings, Biomaterials, 21 (2000) pp. 1339–1343

[7] Z. L. Dong, K. A. Khor, C. H. Quek, T. J. White, P. Cheang, TEM and STEM analysis on heat-treated and in vitro plasma-sprayed hydroxyapatite/Ti-6Al-4V composite coatings, Biomaterials, 24 (2003) pp. 97–105

[8] Chenge Zhang, Yang Leng, Jiyong Chen, Elastic and plastic behavior of plasma-sprayed hydroxyapatite coatings on a Ti–6Al–4 V substrate, Biomaterials, 22 (2001) pp. 1357–1363

[9] Y.C. Yang, Edward Chang, Influence of residual stress on bonding strength and fracture of plasma-sprayed hydroxyapatite coatings on Ti}6Al}4V substrate, Biomaterials, 22 (2001) pp. 1827– 1836

[10] T.M. Sridhar, T.K. Arumugam, S. Rajeswari, M. Subbaiyan, Electrochemical behaviour of hydroxyapatite-coated stainless steel implants, Journal of Materials Science Letters, 16, 23 (1997) pp. 1964-1966

[11] Yong liu, Xiaohong Dan, Yong Du, Fang Liu, Novel coating technique for preparation of hydroxyapatite/Ti composite, Journal of Materials Science, 39, 12 (2004) pp. 4031-4034

[12] Chi-Min Lin, Shiow-Kang Yen, Characterization and bond strength of electrolytic HA/Ti$_{O2}$ double layers for orthopaedic applications, Journal of Materials Science: Materials in Medicine, 16, 10 (2005) pp. 889-897

[13] Stout KJ, Sullivan PJ, Dong WP, et al: Techniques and fidelity of data collection, pp. 17 in Stout KJ; Sullivan PJ; Dong WP, et al. (eds): The development of methods for the characterisation of roughness in three dimensions, University of Birmingham, Commission of the European Communities, Birmingham, UK, 1993

[14] Harold Philip Klug, Leroy E. Alexander Klug, X-ray Diffraction Procedures, Wiley, New York, 1974

[15] S.M.A. Shibli, A.C. Jayalekshmi, Development of phosphate inter layered hydroxyapatite coating for stainless steel implants, Applied Surface Science 254, 13 (2008) pp.4103–4110

[16] Horcas, R. Fernandez, J.M. Gomez-Rodriguez, J. Colchero, J. Gomez-Herrero, A.M. Baro, A software for scanning probe microscopy and a tool for nanotechnology, Rev. Sci. Instrum. 78 (2007) pp. 013705

[17] L. Capitanu, The orthopaedical endoprostheses durability, BREN , Bucharest, 2004 (in Romanian)

[18] D Najjar, A Behnamghader, A. Iost, H. Migaud, Influence of a foreign body on the wear of mrtallic femoral heads and polyethylene acetabular cups of total hip prostheses, Journal of Materials Science: Materials in Medicine, 35 (2000) pp. 4583-4588

[19] L. L. Badita, P. Beca, L. Capitanu, Tribological Characteristics Improvements of Hip Prostheses Using Nanostructured Coatings, 3rd ICMEN Proceedings, 2008, 893 – 902.